Dysfunctional Transforming Growth Factor-β Receptor II Accelerates Prostate Tumorigenesis in the TRAMP Mouse Model

Hong Pu,[1] Joanne Collazo,[2] Elisabeth Jones,[1] Dustin Gayheart,[1] Shinichi Sakamoto,[1] Adam Vogt,[3] Bonnie Mitchell,[3] and Natasha Kyprianou[1,2,3,4,5]

Departments of [1]Surgery/Urology, [2]Toxicology, [3]Pathology, and [4]Molecular and Cellular Biochemistry, and [5]Markey Cancer Center, University of Kentucky College of Medicine, Lexington, Kentucky

Abstract

The contribution of a dysfunctional transforming growth factor-β type II receptor (TGFβRII) to prostate cancer initiation and progression was investigated in an *in vivo* mouse model. Transgenic mice harboring the dominant-negative mutant TGF-β type II receptor (DNTGFβRII) in mouse epithelial cell were crossed with the TRAMP prostate cancer transgenic mouse to characterize the *in vivo* consequences of inactivated TGF-β signaling on prostate tumor initiation and progression. Histopathologic diagnosis of prostate specimens from the TRAMP+/DNTGFβRII double transgenic mice revealed the appearance of early malignant changes and subsequently highly aggressive prostate tumors at a younger age, compared with littermates TRAMP+/Wt TGFβRII mice. Immunohistochemical and Western blotting analysis revealed significantly increased proliferative and apoptotic activities, as well as vascularity and macrophage infiltration that correlated with an elevated vascular endothelial growth factor and MCP-1 protein levels in prostates from TRAMP+/DNTGFβRII+ mice. An epithelial-mesenchymal transition (EMT) effect was also detected in prostates of TRAMP+/DNTGFβRII mice, as documented by the loss of epithelial markers (E-cadherin and β-catenin) and up-regulation of mesenchymal markers (N-cadherin) and EMT-transcription factor *Snail*. A significant increase in the androgen receptor mRNA and protein levels was associated with the early onset of prostate tumorigenesis in TRAMP+/DNTGFβRII mice. Our results indicate that *in vivo* disruption of TGF-β signaling accelerates the pathologic malignant changes in the prostate by altering the kinetics of prostate growth and inducing EMT. The study also suggests that a dysfunctional TGFβRII augments androgen receptor expression and promotes inflammation in early stage tumor growth, thus conferring a significant contribution by TGF-β to prostate cancer progression. [Cancer Res 2009;69(18):7366–74]

Introduction

Approximately 30,000 American men lose their lives due to prostate cancer every year (1). Prostate cancer is a heterogeneous cancer with a natural history of progression from prostatic intraepithelial neoplasia to locally invasive androgen-dependent to androgen-independent metastatic disease, which is associated with increased patient mortality (2). Overcoming the androgen independence of prostate tumors is considered the most critical therapeutic end point for improving patient survival (3). Evidence from *in vitro* studies supports a dynamic contribution of androgen receptor (AR) cross-talk with transforming growth factor-β (TGF-β) signaling toward the emergence of androgen-resistant prostate cancer (4). AR overexpression is an effective way of hormone refractory prostate tumors to overcome the growth inhibition effects of elevated serum TGF-β levels, even in the absence of DHT (4).

TGF-β is a ubiquitous growth factor that elicits diverse cellular responses in cell type–dependent context during different stages of normal development and tumor growth. Disruption of TGF-β signaling correlates with pathologic manifestation of prostatic intraepithelial neoplasia and prostate cancer development (5, 6). Emergence of androgen-independent and metastatic tumors is associated with modulations in activity and/or deregulation of expression of key apoptosis, proliferation, and migration proteins, such as AR, bcl-2, and β-catenin (7–10). AR modulates TGF-β/Smad signaling in androgen-independent prostate tumors by directly antagonizing the growth inhibitory function of TGF-β/Smad signaling (11–13), whereas TGF-β may inhibit AR action via targeting binding of Smad proteins to AR (14, 15). TGF-β signaling proceeds via transmembrane heterotetrameric complexes from two types of serine threonine kinase receptors, type I (TGFβRI) and type II (TGFβRII; ref. 5). Upon ligand binding, TGFβRII receptor phosphorylates and activates TGFβRI receptor, which initiates the downstream signaling cascade by phosphorylating the receptor-regulated Smads (16). Deregulation of TGF-β signaling plays a key role in the pathogenesis of cancer and other diseases, due to either loss of expression or mutational inactivation of its membrane receptors or intracellular effectors, the Smads (6). Loss of responsiveness to TGF-β by introducing a dominant negative mutant TGβRII receptor induces malignant transformation of nontumorigenic rat prostate epithelial cells (17). Overexpression of TGFβRII in prostate cancer cells restores TGF-β sensitivity and suppresses prostate tumorigenic growth (18, 19).

The transgenic adenocarcinoma of mouse prostate (TRAMP) model is transgenic for the SV40 large T antigen under the control of the rat probasin promoter (20, 21). T antigen transgene expression occurs with sexual maturity and results in prostate cancer development and progression in a pattern resembling the clinical progression of human prostate cancer from androgen independence to metastasis (22, 23). To determine the consequences of a dysfunctional TGF-β signaling via loss of TGFβRII on prostate cancer progression, the dominant negative TGFβRII (DNTGFβRII) transgenic mouse model (24) in which TGFβ signaling is impaired via the expression of a DNTGFβRII in

Note: Supplementary data for this article are available at Cancer Research Online (http://cancerres.aacrjournals.org/).

Requests for reprints: Natasha Kyprianou, Division of Urology, MS283, University of Kentucky Medical Center, 800 Rose Street, Lexington, KY 50536. Phone: 859-323-9812; Fax: 859-323-1944; E-mail: nkypr2@uky.edu.

doi:10.1158/0008-5472.CAN-09-0758

epithelial cells, was crossed with the TRAMP mouse. The truncated version of human TGFβRII dimerizes with TGFβRI, but prevents its activation, because it lacks the COOH terminus kinase domain resulting in an inactive TGF-β signaling (24). Here, we generated and characterized a double transgenic TRAMP+/DNTGFβRII mouse model. We found that TGFβRII inactivation in prostate epithelial cells *in vivo* causes an earlier onset of prostate cancer consequential to enhanced growth, vascularity, and inflammation of the prostate.

Materials and Methods

Mice

Animals were maintained under environmentally controlled conditions and subject to a 12-h light/dark cycle with food and water *ad libitum*. Animals (six to eight mice per group) were divided into the following experimental groups: (*a*) TRAMP+/DNTGFβRII+, (*b*) TRAMP+/WtTGFβRII, (*c*) TRAMP−/DNTGFβRII+, and (*d*) TRAMP−/WtTGFβRII. For immunohistochemical analysis, prostate tissue specimens were fixed in 10% (v/v) formalin (Sigma-Aldrich), and formalin-fixed paraffin-embedded tissue specimens were sectioned (6 μm) using a Finesse microtome (Thermo Shandon, Inc.).

Characterization of DNTGF-β RII Transgenic Conditional Knockout Mice

The DNTGFβRII mice were obtained from Dr. Lalage Wakefield (National Cancer Institute, Bethesda, MD). The DNTGFβRII transgene contains three different integrations of a construct that has a truncated version of the human TGFβRII expressed under the control of a mouse metallothionein MT1 (induced by $ZnSO_4$ in drinking water) and metallothionein locus control regions (25). Metallothioneins are low molecular weight, cysteine-rich proteins, which expression is rapidly induced in response to cadmium and zinc. The DNTGFβRII transgene mouse is in the FVB/N genetic background (24). By crossing the original DNTGFβRII+/+ transgenic female mice (Background FVB) with wild-type C57BL/6 male mice for six generations, DNTGFβRII± in the C57BL/6 background mice have been generated. Transgenic mice were identified by PCR. For DNTGFβRII, genotyping PCR conditions were as follows: 30 cycles, 60 s, 94°C, 60 s, 56°C; 60 s 72°C. Forward primer: 5′-AAGATGATGTTGTCATTGCACTC-3′; reverse primer: 5′-TGGAGAAAGAATGACGAGAACA-3′ yield a 183-bp PCR product.

Generation of TRAMP/DNTGFβRII Transgenic Mice

The TRAMP mouse model (C57BL/6-Tg-TRAMP-8247Ng; Jackson Laboratory) is a well-established model of prostate cancer progression to advanced disease. The TRAMP transgene is in the C57BL/6 genetic background. TRAMP was detected by PCR using the following specific primers: TRAMP forward primer, 5′-CAGAGCAGAATTGTGGAGTGG-3′; TRAMP reverse primer, 5′-GGACAAACCACAACTAGAATGCAGTG-3′, a 489-bp product. PCR conditions: 25 cycles 60 s; at 95°C, 60 s at 55°C, and 60 s at 72°C. DNTGFβRII heterozygous males in the C57BL/6 background were crossed to TRAMP heterozygous females (of same background). Male mice (C57BL/6) of the following genotypes were thus generated as follows: TRAMP+/DNTGFβRII+, littermates TRAMP+/WtTGFβRII; TRAMP−/DNTGFβRII+, and TRAMP−/WtTGFβRII to serve as controls.

Truncated Version of Human DNTGFβRII mRNA and Protein Expression Induced by $ZnSO_4$

Reverse transcription-PCR (RT-PCR) was used to determine DNTGFβRII receptor mRNA levels in TRAMP+/DNTGFβRII+ and littermates TRAMP+/WtTGFβRII; TRAMP−/DNTGFβRII+; TRAMP−/WtTGFβRII transgenic mice (with and without 25 mmol/L $ZnSO_4$ in drinking water). Total RNA (TRIzol; Invitrogen) was reverse transcribed using Promega Corporation kit. Transcription conditions were as follows: 25°C for 10 min, 42°C for 60 min, and 95°C for 5 min. Primer forward: 5-CAC TGA CAA CAA CGG TGC AGT C-3. Primer reverse: 5-GCA ACA AGT CAG GAT TGC TGG TG-3. The expected PCR product was a 372-bp fragment. Quantum mRNA 18 s (Ambion, Inc.) was used as an internal control. Thermocycling conditions were as follows: 94°C, 1 min before the first cycle, 94°C, 30 s, 56°C, 30 s, and 72°C, 30 s, for 36 times and followed by a final extension at 72°C, 7 mins. PCR products were separated in 2% agarose gels, stained with ethidium bromide (Invitrogen), and visualized using UVP Bioimaging system (UVP LCC). The band intensity was quantified using Scion image analysis software (Scion Corporation).

Paraffin sections (6 μm) were deparaffinized, rehydrated, and stained with H&E and were subjected to pathologic evaluation by the pathologist (BM). To examine DNTGFβRII protein expression, formalin-fixed paraffin-embedded sections of mouse prostates were deparaffinized and subjected to antigen retrieval in citrate buffer (pH 6; Dako); slides were rinsed with TBS containing 0.05% Tween 20 [50 mmol/L Tris, 150 mmol/L NaCl (pH 7.6) and 0.1% (v/v) Triton X-100], and subsequently exposed to the rabbit polyclonal antibody against human TGFβRII (Upstate; 4°C; overnight). Negative controls consisted of exposing tissue sections to rabbit IgG (Santa Cruz Biotechnology). Slides were incubated with biotinylated goat anti-rabbit IgG (Chemicon; 1 h at room temperature) and subsequently exposed to streptavidin-conjugated Texas red (Chemicon). Slides were examined under a Nikon fluorescence microscope (Nikon, Inc.).

Apoptosis Detection

The incidence of apoptosis was examined *in situ* using the terminal deoxynucleotidyl transferase-mediated dUTP-biotin nick end labeling (TUNEL) assay (Chemicon International). Sections were counterstained with methyl green and TUNEL-positive cells were counted (26). The apoptotic index was expressed as the percentage of TUNEL-positive cells over the total number of cells in three random fields (×40).

Evaluation of Cell Proliferation, Vascularity, Inflammation, and Epithelial-Mesenchymal Transition

Cell proliferation, tissue vascularity, macrophage recruitment, and epithelial-mesenchymal transition (EMT) markers, as well as AR expression were determined by immunohistochemical and Western blot analysis.

Immunohistochemical analysis. The antibodies used were as follows: the rabbit polyclonal antibody against mouse E-cadherin (Cell Signaling Technology, Inc.), N-cadherin, AR, and mouse TGFβRII (Santa Cruz Biotechnology); the antibody against nuclear antigen Ki-67 (Abcam, Inc.) was used as a marker of proliferation; the rabbit polyclonal antibody against mouse von Willebrand Factor (vWF; Dako) was used to evaluate microvessel density as an indicator of tissue vascularity; the rat anti-mouse CD68 (Abd Serotec) was used to detect macrophage infiltration. Citrate buffer and proteinase K solution (20 μg/mL) was used for vWF antigen retrieval. Serial sections were exposed to Ki-67, AR, vWF, and CD68 antibodies, overnight at 4°C (negative controls consisted of incubation with IgG from the host of primary antibody). Sections were subsequently exposed to biotinylated goat anti-rabbit IgG and horseradish peroxidase–streptavidin conjugate (Chemicon). Color development was accomplished using a FAST 3, 3-diaminobenzidine–based kit (Sigma-Aldrich), and counterstained with hematoxylin. Images were captured using an Olympus BX51 microscope system (Olympus America). The number of Ki-67 positive cells over total number of prostate epithelial cells (300–500) was counted two independent observers.

Western Blot Analysis

Prostate tissue was homogenized in TRIzol Reagent and protein was extracted following the manufacturer's instructions. Protein expression was determined by immunoblotting using the following specific antibodies: anti–vascular endothelial growth factor (VEGF; Santa Cruz Biotechnology), anti MCP-1, and anti-Snail (Cell Signaling Technology); anti–E-cadherin, anti–N-cadherin, anti-mouse TGFβRII (same as described above for immunohistochemical analysis), and anti β-catenin (Cell Signaling Technology). Protein levels were normalized to α-actin expression, using the α-actin antibody (Oncogene Research Products). Protein content was quantified using the bicinchoninic acid (Pierce) and protein samples (30 μg) were subjected to SDS-PAGE and transferred to Hybond-C membranes (Amersham Pharmacia Biotech). Membranes were blocked in 5% milk in TBS containing 0.05% Tween 20, and following incubation with the

respective primary antibody (overnight at 4°C), membranes were exposed to species-specific horseradish peroxidase–labeled secondary antibody. Signal detection was achieved with SuperSignal West Dura Extended Duration Substrate (Pierce) and visualized using a UVP Imaging System. Fold change was determined based on α-actin expression as a control.

Real-time PCR Analysis

Real-time RT-PCR was used to determine TGF-β, AR, Bax, Bad, p21, and mouse TGFβRII mRNA expression. Total RNA was extracted from prostate tissue using the TRIzol Reagent (Invitrogen), and 1 μg RNA was reverse transcribed using a Promega kit according to the following conditions: 25°C for 10 min, 42°C for 60 min, and 95°C for 5 min. Inventoried Primer pairs and TaqMan probes (Applied Biosystems) were used to determine TGF-β and AR mRNA levels. Real-time PCR was conducted on an ABI Prism 7300 system, in TaqMan Universal PCR Master Mix, primers (95°C for 10 min, followed by 95°C, 15 s and 60°C, 60 s). Numerical data (normalized to 18 SmRNA levels) indicate mean values ± SEM, n = 6-8.

Statistical Analysis

The data presented on Table 1 were analyzed for statistical significance using the unpaired t test. Results from all other experiments were analyzed by one-way ANOVA followed by Tukey's and Dunn's test using the SigmaStat 2.03 program (SPSS). Numerical values are expressed as the mean ± SEM. Statistical differences were considered significant at P value of <0.05.

Results

DNTGFβRII Expression in Prostates from Double Transgenic TRAMP+/DNTGβRII Mice

By crossing heterozygous DNTGFβRII+/− mice in the C57BL/6 background with heterozygous TRAMP mice in the same background, we generated the following transgenic mice: TRAMP+/DNTGFβ RII (Fig. 1*A, lanes 4* and *7*), TRAMP+/WtTGFβRII (Fig. 1*A, lanes 6* and *9*), and their control litters: TRAMP−/DNTGFβRII (Fig. 1*A*, lanes *1, 2, 3, 5*, and *11, 5*) and TRAMP−/WtTGFβRII (Fig. 1*A, lanes 8* and *10*). RT-PCR revealed that DNTGFβRII gene expression is successfully turned on in the prostate of TRAMP+/DNTGFβRII (Fig. 1*B, lane 2*) and TRAMP−/DNTGFβRII mice (Supplementary Fig. S2*I*) after 29 days on 25 mmol/L $ZnSO_4$. Lower levels of mRNA DNTGFβRII were detected in the prostates of TRAMP+/DNTGFβRII (Fig. 1*B, lane 3*) and TRAMP−/DNTGFβRII (Supplementary Fig. S2*I*) without $ZnSO_4$. Prostate mRNA DNTGFβRII expression in TRAMP+/DNTGFβRII was higher under zinc-induction (Fig. 1*C*). DNTGFβRII protein was detected using immunohistochemical staining (24). As shown on Fig. 1*D*, cell membrane DNTGFβRII expression was localized in prostate epithelial cells from TRAMP+/DNTGFβRII mice (*top*).

To test the consequences of the exogenous DNTGFβRII on normal TGFRII expression in relation to DNTGFRII, we determined the expression of mouse endogenous wild-type TGFβRII and the main TGFβ signaling downstream mediator p21, in control mice (TRAMP−,12 weeks), in the absence or presence $ZnSO_4$. Mechanistically, the transgenic DNTGFβRII is expected to compete with original wild-type TGFβRII, without affecting the expression of the latter in the TRAMP mouse. We found a slight increase in mouse wild-type TGFβRII mRNA, but no significant difference in the expression of mouse wild-type TGFβRII and DNTGFβRII positive mice at the mRNA level (Supplementary Fig. S1*I*). Nor there was a significant difference in p21 mRNA between the DNTGFβRII and

Table 1. Histopathological evaluation of prostate tumors in double transgenic TRAMP/DNTGFβRII mice

A. Tumor grade evaluation of prostate TRAMP tumors with DNTGFβRII vs TRAMP mice with wild-type TGFβRII littermates

	12 wk	16 wk	20 wk	24 wk	Control (20 wk TRAMP −)
	TRAMP+/Wt TRAMP+/DN	TRAMP+/Wt TRAMP+/DN	TRAMP+/Wt TRAMP+/DN	TRAMP+/Wt TRAMP+/DN	TRAMP+/Wt TRAMP+/DN
Anterior	3.00 ± 0.00 3.50 ± 0.41	3.33 ± 0.29 4.17 ± 0.29	3.67 ± 1.16 5.33 ± 0.76*	3.75 ± 0.35 4.50 ± 1.32	1.83 ± 0.50 2.17 ± 0.29
Dorsal+lateral	3.17 ± 0.29 3.57 ± 0.29	3.67 ± 0.58 4.67 ± 0.58	4.33 ± 0.58 5.00 ± 0.71	4.67 ± 0.76 5.33 ± 0.58	1.83 ± 0.58 2.16 ± 0.29
Ventral	2.00 ± 0.00 2.17 ± 0.29	3.00 ± 0.00 3.33 ± 0.58	3.17 ± 0.29 3.33 ± 0.58	2.67 ± 0.29 3.00 ± 0.50	1.50 ± 0.50 2.17 ± 0.29

B. Quantitative analysis of prostate apoptosis, proliferation, vascularity, and inflammation

		Ki67 staining	Apoptosis	Vessel	Macrophage
12 wk	TRAMP+/Wt	24.84 ± 2.89	4.52 ± 0.67	2.00 ± 1.00	5.00 ± 0.58
	TRAMP+/DN	28.81 ± 2.09	8.96 ± 0.64 †	2.33 ± 1.15	5.60 ± 0.67
16 wk	TRAMP+/Wt	44.73 ± 6.65	5.37 ± 0.50	3.00 ± 2.00	12.33 ± 1.45
	TRAMP+/DN	52.22 ± 6.97	7.35 ± 1.00	2.70 ± 1.50	25.33 ± 5.04 †
20 wk	TRAMP+/Wt	38.94 ± 5.05	5.55 ± 1.89	3.33 ± 0.58	18.67 ± 1.45
	TRAMP+/DN	53.86 ± 2.61 †	14.88 ± 1.23 †	3.66 ± 0.58	36.67 ± 4.63 †
24 wk	TRAMP+/Wt	42.56 ± 4.89	8.56 ± 2.19	3.70 ± 1.53	55.67 ± 4.98
	TRAMP+/DN	43.99 ± 3.23	13.92 ± 2.33	4.00 ± 1.00	88.33 ± 8.41 †

NOTE: Numerical values are the mean ± SD (n = 6–8 mice/group). Values shown are the mean ± SEM (n = 6–8 mice/group). The prostates from TRAMP-negative control littermates exhibited occasional Ki67, apoptosis, and macrophage-positive cells (Supplementary Table S1).

*A significant difference between the TRAMP+/DNTGFβRII+ and TRAMP+/WtTGFβRII in 20-wk mice (P < 0.05).

†A significant difference between the TRAMP+/DNTGFβRII+ and TRAMP+/WtTGFβRII (P < 0.05).

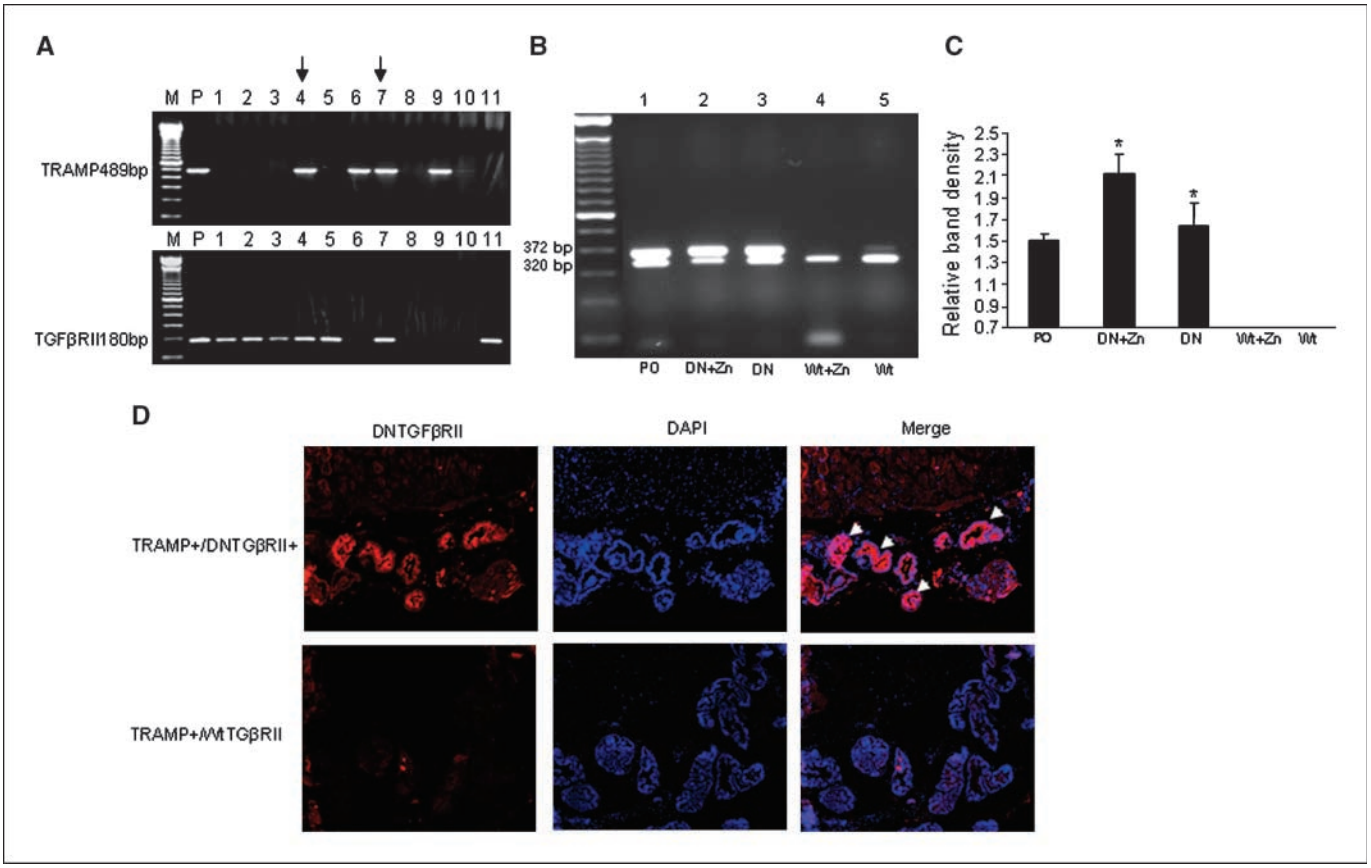

Figure 1. *A,* genotype characterization of TRAMP+/DNTGFβRII transgenic mice. *Lane P,* positive control; *lanes 4* and *7*, TRAMP+/DNTGFβRII mice; *lanes 6* and *9,* TRAMP+/WtTGFβRII mice and control litters: TRAMP−/DNTGFβRII (*lanes 1, 2, 3, 5*, and *11*) and TRAMP−/WtTGFβRII (*lanes 8* and *10*). *B,* RT-PCR of DNTGFβRII transgenic gene expression in the prostate. *Lane 1,* positive control. *Lanes 2* and *3,* prostate mRNA from 12-wk-old TRAMP+/DNTGFβRII mice in the presence and absence of 25 mmol/L $ZnSO_4$. *Lanes 4* and *5,* prostates from 12 wk-old TRAMP+/WtTGFβRII mice. *Upper bands,* DNTGFβ RII 372 bp. *Lower bands,* comp timer internal control 18 S 320 bp. *C,* band intensity for DNTGFβ RII was normalized to 18 S. *D,* DNTGFβRII immunofluorescence using an anti-DNTGFβRII (*red*) antibody and 4′,6-diamidino-2-phenylindole (*DAPI*; *blue*) for nuclear staining. *Top,* prostate from a 12-wk TRAMP+/DNTGFβRII mouse in presence of 25 mmol/L $ZnSO_4$.

wild-type TGFβRII mice (Supplementary Fig. S1). The modest increase in wild-type TGFβRII protein was observed in DNTGFβRII-positive mice (Supplementary Fig. S1*II* and *III*).

Pathologic evaluation. The results of histopathologic grading of prostatic tumor lesions using a standard grading scale in TRAMP mice (27) are shown in Supplementary Fig. S3 (Supplementary Data). A semiquantitative analysis of lesion distribution in all lobes of prostate is presented in Table 1*A*. TRAMP-negative mice (20-week-old) were used as controls. Flat lesions (grade 1–1.8) were observed in the majority of littermates TRAMP−/Wt TGFβRII mice (Supplementary Fig. S3*A*, 20 weeks; Table 1*A*). Flat lesions and focal cell piling (grade 2–2.5) were detected in the 20-week-old control TRAMP−/DNTGFβRII+ mice (Supplementary Fig. S3*B*), indicating that DNTGFβRII mice have potential for earlier development of hyperplastic lesions. In 12-week TRAMP mice, histologic analysis revealed focal cribriform lesions protruding into the lumen (grade 3) occurred in the anterior lobes of TRAMP+/DNTGFβRII+ and TRAMP+/WtTGFβRII mice. At 16 weeks of age, TRAMP+/DNTGFβRII+ mice developed neuroendocrine type adenocarcinoma with local invasion (grade 6), in the prostate lateral lobe (Supplementary Fig. S3*F*).

In the ventral prostates, papillary lesions protruding into lumen (grade 2–3) were detected in TRAMP+/WtTGFβRII and TRAMP+/DNTGFβRII+ mice (Table 1*A*). The anterior prostate lobes in both groups of mice, exhibited regions of focal epithelial hyperplasia (Fig. 5*A, e* and *f*). More aggressive focal epithelial hyperplasia was expressed in TRAMP+/DNTGFβRII+ mice (Fig. 5*A, f*). The anterior prostate lobes of TRAMP+/DNTGFβRII+ mice exhibited grades 4 to 5 (Table 1). Lesions in TRAMP+/DNTGFβRII+ mice were more advanced than in TRAMP+/WtTGFβRII mice, exhibiting distinct grade 5 intraluminal masses that expanded the acini in dorsal lobes (Supplementary Fig. S3*C* and *D*). Histologic diagnosis indicated that relative to TRAMP mice with intact TGFβRII signaling, prostate tumor lesions in the TRAMP+/DNTGFβRII+ mice are more severe over 12 to 24 weeks in the anterior and dorsal-lateral lobes. Ventral lobes showed reduced tumor progression with aging compared with the other lobes in dysfunctional and intact TGFβRII TRAMP mice (Supplementary Fig. S3).

Consequences of disrupted TGFβRII on prostate cell proliferation and apoptosis in TRAMP mice. The DNTGFβRII led to an increased proliferative index at each stage of progression (12, 16, 20, 24 weeks of age; Fig. 2*A*). This was paralleled by an increase in the apoptotic cells in TRAMP+/DNTGβRII+, compared with TRAMP+/Wt TGFβRII (Fig. 2*B*). The prostate proliferative index in TRAMP+/DNTGFβRII+ mice was higher compared with control TRAMP+/Wt TGFβRII mice at respective ages, 12, 16, 20, and 24 weeks (Table 1*A*). The prostate cell apoptotic index was also higher in the TRAMP+/DNTGβRII+ prostates compared with the

TRAMP+/WtTGFβRII mice (Table 1*B*). To dissect this elevated apoptosis, we examined the expression of key proapoptotic effector players Bax and Bad. As shown on Fig. 2*C*, bax gene expression was up-regulated in 20-week-old TRAMP+/DNTGβRII, compared with TRAMP+/WtTGFβRII. There was also an increase detected for bad mRNA, but this failed to reach a statistical significant difference (Fig. 2*C*).

Prostate Vascularity and Inflammation in Transgenic DNTGFβRII/TRAMP Mice

To investigate whether increased tumorigenicity of TRAMP+/DNTGFβRII+ was associated with increased angiogenesis, vWF-immunostaining was examined (Fig. 3*A*). There was no significant difference in the vascularity of prostate stroma between TRAMP+/DNTGFβRII+ and TRAMP+/WtTGFβRII (Table 1*A*) and their littermate mice (Supplementary Fig. S2). However, there was increased intensity of neo-capillary–like vessels observed in prostate tumor regions of TRAMP+/DNTGFβRII (Fig. 3*A, f, g, h, i*, and *j*) compared with controls (Fig. 3*A, a, b, c, d*, and *e*). An increase in VEGF protein levels was detected in TRAMP+/DNTGFβRII prostates (Fig. 3*C*). There was also an increase in macrophage infiltration into prostate tumors from TRAMP+/DNTGFβRII+ compared with TRAMP+/WtTGFβRII mice detected at 16, 20, and 24 weeks (Fig. 3*B*). CD68-positive cells were abundant in prostate stroma in TRAMP mice (12–24 weeks). With advancing age (>24 weeks), prostate glands of TRAMP+/DNTGFβRII+ mice exhibited strong luminal CD68-immunoreactivity (Fig. 3*A, j*). Moreover, there was a marked increase in the MCP-1 protein levels in prostate tissue from the TRAMP+/DNTGFβRII that directly correlated with high macrophage detection (Fig. 3*D*).

EMT-like Pathologic Change in Transgenic TRAMP/DNTGFβRII Mice

Reduced E-cadherin and increased N-cadherin expression are recognized characteristic features of EMT. Figure 4*A* reveals characteristic E-cadherin and N-cadherin immunoreactivity in prostate from TRAMP+/DNTGFβRII and TRAMP+/WtTGFβRII mice. Reduced E-cadherin immunoreactivity was detected in 12- and 16-week-old TGFβRII transgenic (Fig. 4*A, b* and *d*) compared with wild-type TGFβRII (Fig. 4*A, a* and *c*) TRAMP mice. E-cadherin immunoreactivity was lost (Fig. 4*A, e* and *f*) in 20-week TRAMP+/DNTGFβRII. Moderately differentiated prostate tumors detected in the lateral prostates of 24-week TRAMP+/DNTGFβRII lack E-cadherin, whereas well-differentiated prostate tumors from age-matched TRAMP+/WtTGFβRII exhibited strong E-cadherin immunoreactivity (Fig. 4*B, e* and *f*). The higher density of N-cadherin–positive myofibroblast-like cells extended into prostate tumor were observed in the TRAMP+/DNTGFβRII mice (Fig. 4*B, b, d, f*, and *h*), compared with TRAMP+/WtTGFβRII mice (Fig. 4*B, a, c, e*, and *g*). Mechanistic profiling revealed down-regulation of epithelial markers, E-cadherin, β-catenin, and up-regulation of the mesenchymal marker N-cadherin and Snail, an EMT player, in TRAMP+/DNTGFβRII prostates (Fig. 4*C* and *D*).

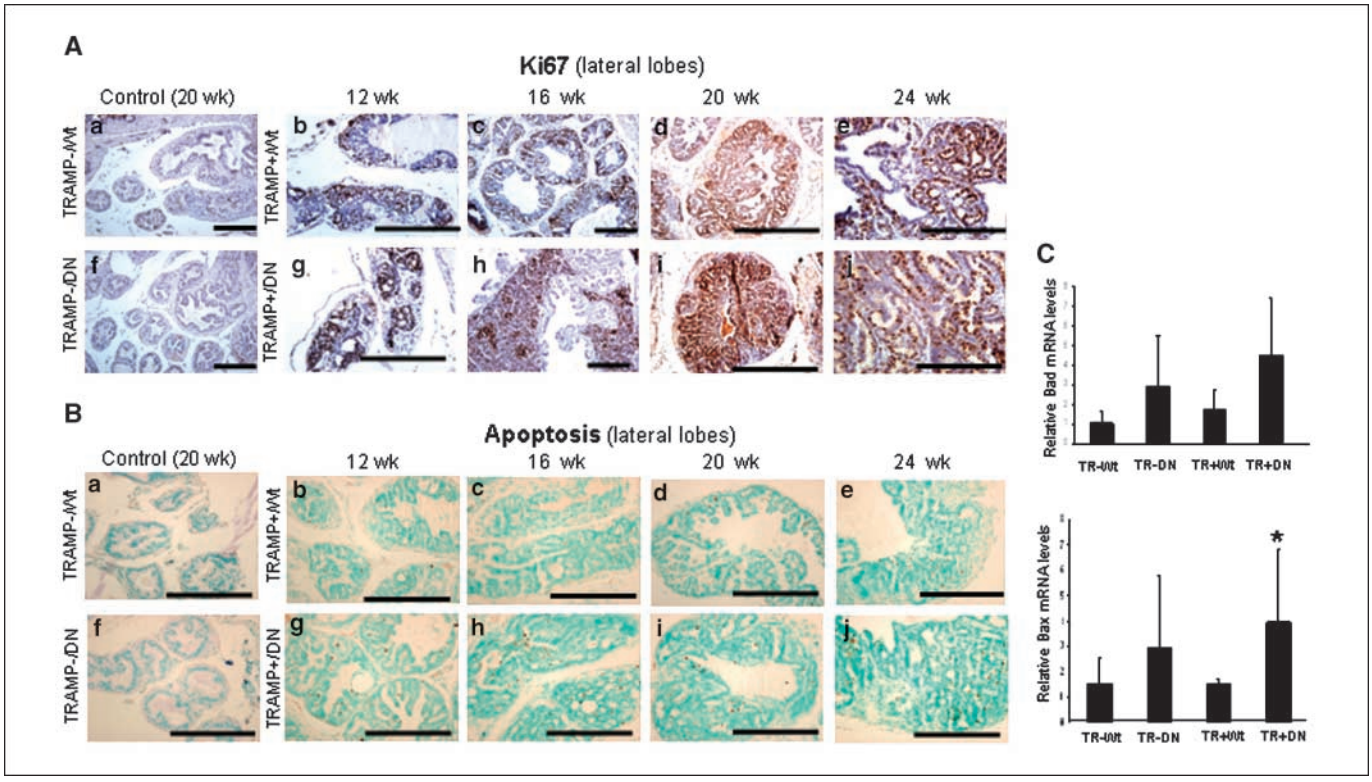

Figure 2. Prostate cell proliferation and apoptosis in TRAMP+/DNTGFβRII, TRAMP+/WtTGFβRII, and control littermates. *A,* Ki-67 immunostaining and hematoxylin counterstaining (*blue*) were performed in prostates from 12, 16, 20, and 24-wk mice (on $ZnSO_4$ for 45 d). Prostate tissue from controls (20 wk), TRAMP−/WtTGFβRII, and TRAMP−/DNTGFβRII mice with low Ki-67 staining is shown on *a* and *f. b, c, d*, and *e,* Ki-67 immunostaining of TRAMP+/WtTGFβRII prostates (12–24 wkage). *g, h, i*, and *j,* Ki-67 staining of TRAMP+/DNTGFβRII+ mice of the same age range. *B,* detection of TUNEL-positive cells; counterstaining with methyl green in prostates from 12- to 24-wk-old mice. Prostates from TRAMP−/WtTGFβRII and TRAMP−/DNTGFβRII+ mice exhibited fewer apoptotic cells (*a* and *f*). *b, c, d*, and *e,* TUNEL staining in prostates from TRAMP+/WtTGFβRII mice (12–24 wk). *g, h, i*, and *j,* apoptotic cells. *C,* real-time RT-PCR was used to analyze Bad and Bax mRNA expression in prostates from TRAMP+/DNTGFβRII+, TRAMP+/WtTGFβRII mice, and control littermates (20 wk). *, significantly different in TRAMP+/DNTGFβRII+ compared with TRAMP+/WtTGFβRII. $P < 0.05$.

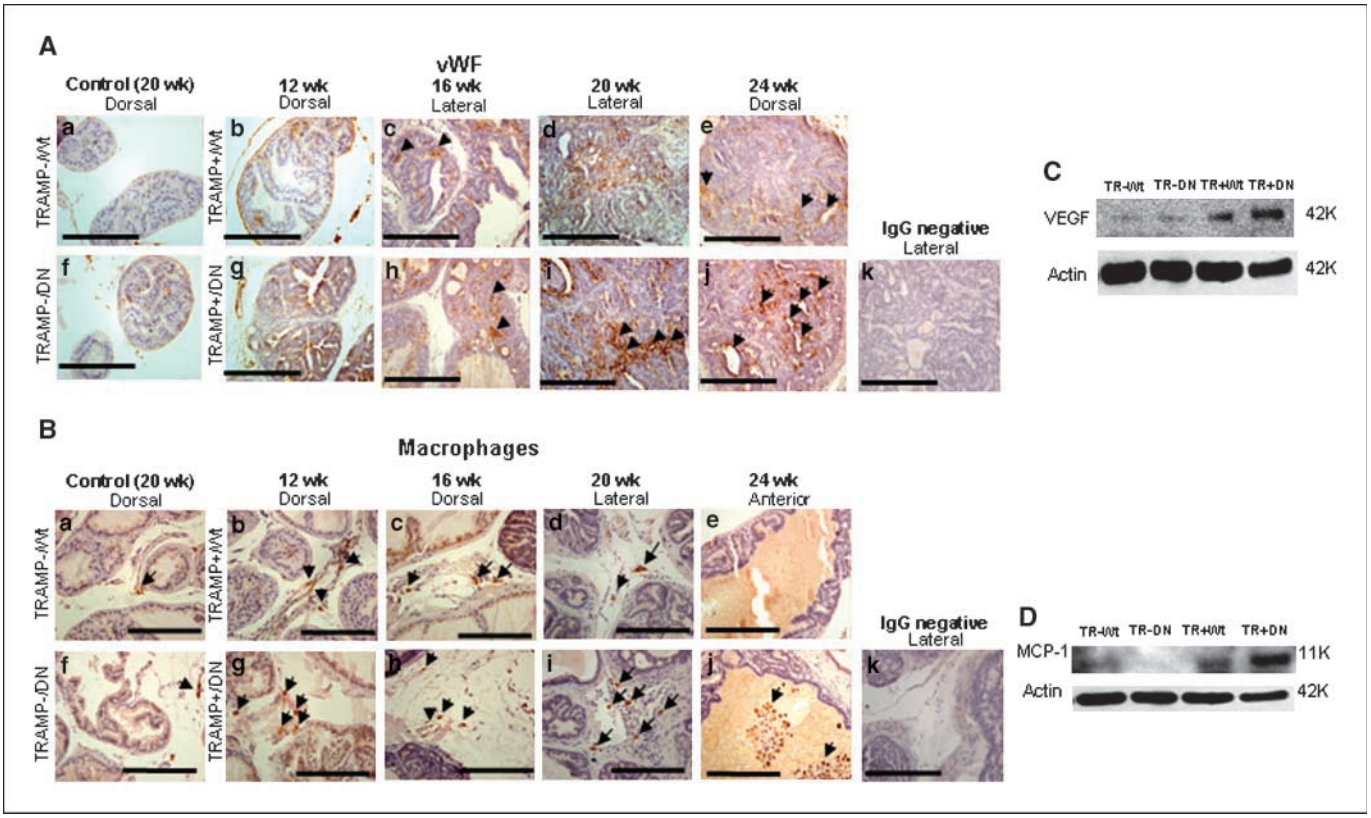

Figure 3. Microvessel density and macrophage infiltration in prostates of TRAMP+/DNTGFβRII+, TRAMP+/WtTGFβRII mice. *A,* immunostaining with anti-vWF antibody and hematoxylin counterstaining (*blue*) were performed in prostate tissue from 12- to 24-wk mice. *a* and *f,* prostates from controls (at 20 wk); *b, c, d*, and *e,* vWF staining of TRAMP+/WtTGFβRII+ mice of increasing ages (12–24 wk). *g, h, i*, and *j,* vWF staining of TRAMP+/DNTGFβRII+ mice (12–24 wk). *k*, negative control IgG staining. *B,* CD68 staining for macrophages (*brown*). Prostates from control mice are shown in *a* and *f. b, c, d*, and *e,* CD68 staining in TRAMP+/WtTGFβRII+ prostates. *g, h, i*, and *j,* CD68 immunoreactivity in prostate with impaired TGF-β signaling. *k,* negative control IgG staining. *C* and *D,* VEGF and MCP-1 protein expression in prostates of TRAMP+/DNTGFβRII+ and control mice (20 wk) was evaluated by Western blotting.

Induction of TGF-β Ligand and AR Expression in DNTGFβRII/TRAMP Prostates

As shown on Fig. 5*A*, the presence of dysfunctional DNTGFβRII receptor resulted in elevated TGF-β ligand mRNA expression. We found a significant upregulation of AR mRNA in TRAMP+/DNTGFβRII transgenic mice compared with TRAMP+/WtTGFβRII and controls (Fig. 5*B*). AR immunoreactivity was primarily of nuclear localization among the prostate epithelial cells (Fig. 5*C*). TRAMP−/DNTGFβRII and TRAMP−/WtTGFβRII–derived prostates exhibited low AR immunoreactivity, whereas a strong AR expression was detected in TRAMP+ prostates. Higher AR expression was detected in TRAMP mice with inactivated DNTGFβRII, compared with TRAMP mice with wild-type TGFβRII, RII, a change that correlated with the AR mRNA increase in prostate epithelial cells of TRAMP+/DNTGFβRII (Fig. 5*C*).

Discussion

Functional defects in TGF-β signaling have been implicated in cancer development and progression (28), but the mechanisms underlying resistance to TGF-β–mediated growth inhibition in prostate cancer cells are not fully understood (29), although TGFβRII mutations are more frequent than TGFβRI mutations (30). This study investigated the temporal involvement of mutational inactivation of TGFβRII in prostate epithelial cells in prostate tumorigenesis. Double transgenic TRAMP+/DNTGFβRII+ mice exhibited pathologic evidence of prostatic intraepithelial neoplasia and poorly differentiated prostate adenocarcinoma at an early age, compared with TRAMP+/Wt TGFβRII mice, indicating that TGF-β signaling triggers abnormal growth kinetics at the onset of prostate cancer development. Our results are in accordance with the role of TGF-β as a tumor suppressor in the early stages of prostate tumorigenesis, and as a tumor promoter in advanced disease (31, 32). Another *in vivo* study engaging the expression of a DNTGFβRII in mouse skeletal tissue reported that disruption of TGF-β signaling led to prostate cancer metastasis, challenging the existing knowledge that TGF-β is strong promoter of cancer metastasis (12). Here, the DNTGFβRII was expressed in mouse epithelial cells, responsible for giving rise to tumor cells in TRAMP mice. One could argue that TGFβRII loss of function in the epithelial cells may increase TGFβ ligand through paracrine effects. Consequently, increased TGF-β levels stimulate nonmalignant stromal cell types of the tumor in angiogenesis, extracellular matrix degradation, and EMT (33–35), leading to tumor invasion and metastasis. This evidence is in accord with our results indicating increased intraprostatic TGF-β mRNA levels to correlate with TRAMP+/DNTGFβRII+ mice.

Recurrence of highly aggressive, metastatic prostate tumors (36–38) due to the emergence of androgen-independent prostate cancer cells results from gene alterations in players regulating androgen-dependent apoptosis of normal prostate epithelium (39). One cannot dismiss the evidence that changes in AR

signaling may also become a contributing factor by using low levels of androgens (40), or by co-opting the AR in other signaling pathways (3, 41–43). TGFβRII has been implicated in the androgenic control of TGF-β signaling in prostate epithelial cells (44). The TGF-β promoter contains three distal and three proximal androgen-response elements that physically interact with the DNA-binding domain of AR (45). In our study, disruption of TGFβRII signaling led to a significant increase of the proliferative index of prostate cancer cells, a change that was paralleled by a significant up-regulation of AR. The present findings resonate with our previous *in vitro* studies (46), supporting the engagement of TGF-β signaling in antiandrogenic properties of prostate cancer cells, via a dysfunctional TGF-β/AR cross-talk. Interestingly, a contextual role of TGF-β in breast cancer was associated with the estrogen receptor status (47).

In our experimental model, DNTGFβRII led to the early manifestation of the aggressive premalignant pathologic characteristics of prostate tumors. TGF-β triggers apoptosis depending on cell-autonomous and environmental factors whose molecular identity remains unknown (48). The increased incidence of apoptosis among the epithelial cells in TRAMP+/DNTGFβRII+ prostates was unexpected and might represent a "feedback" phenomenon under abnormally high proliferative conditions, to which cell growth dynamics react to maintain an appropriate apoptotic rate, counteracting TGF-β signaling. This finding might seem in sharp contrast to the apoptotic role of TGF-β, but nevertheless consistent with the enhanced and frequent apoptosis occurring in hyperplastic lesions of TGFβRII null mammary epithelium (49), as well in high-grade neoplasms (50). Converging oncogenic gene mutations might result in dramatic losses of the normal apoptotic response to TGF-β *in vivo*. Moreover, the microenvironment and immune system enjoy a complex dynamic exchange, regulated by inflammatory cells, extracellular matrix, and degradation and cytokine signaling controlling these processes. Our results indicate that DNTGFβRII expression targets important cellular processes in the prostate epithelial cells, such as leading to enhanced inflammation (via MCP-1 induction and macrophage infiltration), increased vascularity (as shown by increased VEGF), and EMT induction (associated with metastatic progression).

Loss of E-cadherin expression correlated with an increased proliferative rate and tumor aggressiveness in the TRAMP+/DNTGFβRII+ derived prostate tumors. Such a correlation between loss of E-cadherin expression and Gleason grade has been shown in human prostate tumors (51). Cancer cell dedifferentiation via activation of EMT-associated pathways

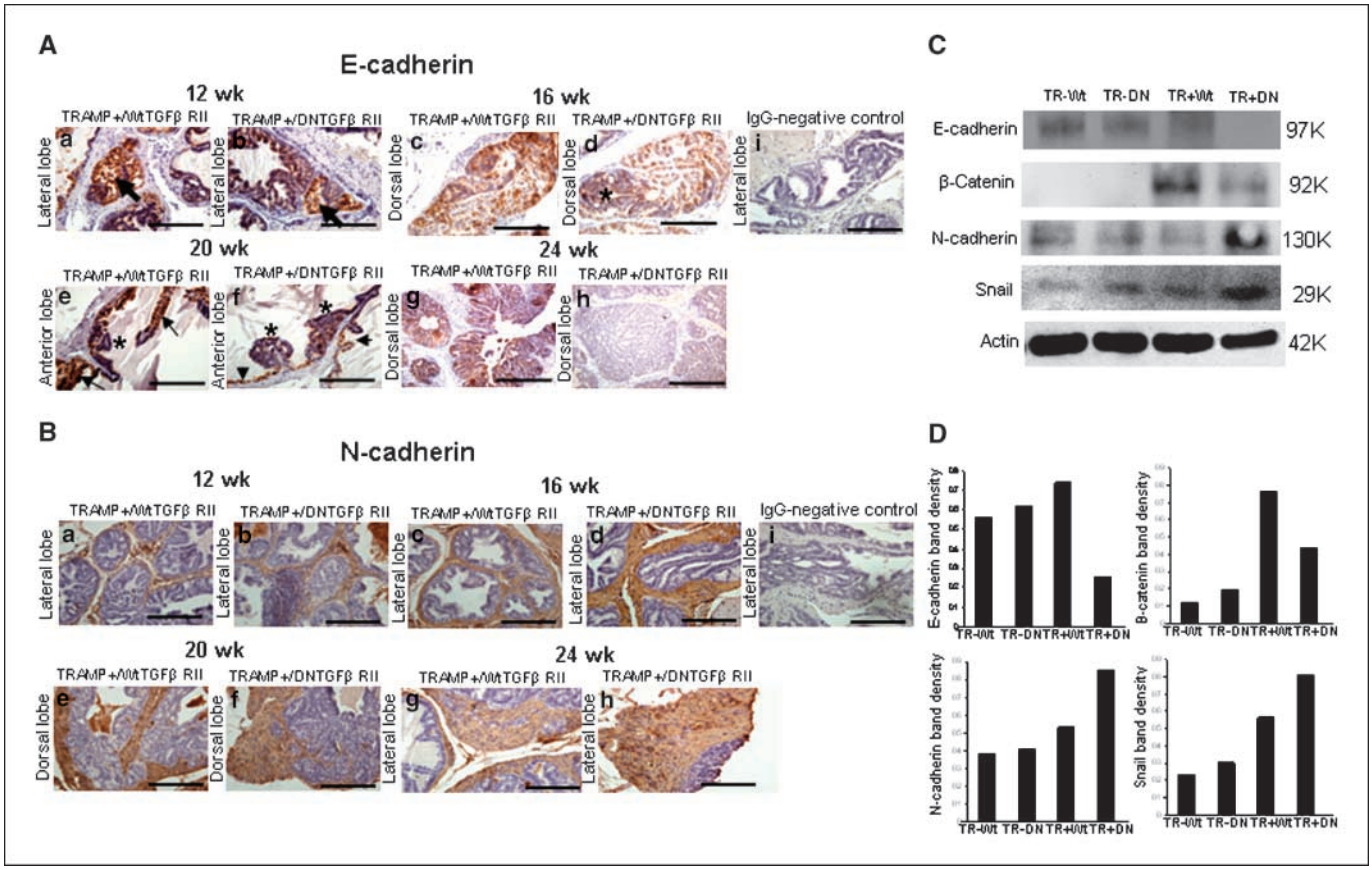

Figure 4. *A,* EMT in prostates with impaired TGF-β signaling. *a* and *b,* E-cadherin immunoreactivity in the lateral lobes of TRAMP+/WtTGFβRII and TRAMP+/DNTGFβRII+ mice (12 wk), respectively. *c* and *d,* E-cadherin immunoreactivity in the dorsal lobes at 16 wk; *e* and *f,* in anterior prostate lobes of WtTGFβRII and DNTGFβRII+ TRAMP mice at 20 wk, respectively. *g* and *h,* E-cadherin expression in dorsal lobes. *Arrow,* E-cadherin–positive cells; *, E-cadherin negative. *B, a* and *b,* N-cadherin immunoreactivity in lateral lobes, TRAMP+/WtTGFβRII and TRAMP+/DNTGFβRII+ mice at 12 wk, respectively. *c* and *d,* N-cadherin immunoreactivity in lateral lobes (16 wk). *e* and *f,* N-cadherin immunoreactivity pattern in the dorsal prostate lobes of WtTGFβRII and DNTGFβRII of TRAMP mice (20 wk), respectively. *g* and *h,* N-cadherin lateral lobe expression. *i*, IgG-negative control. *C,* prostate E-cadherin, N-cadherin, β-catenin, and Snail expression in TRAMP+/DNTGFβRII+, TRAMP+/WtTGFβRII mice, and control littermates (20 wk). Prostate lysates were subjected to Western blotting for E-cadherin, N-cadherin, β-catenin, and *Snail* protein expression. *D,* relative band intensity from *C*.

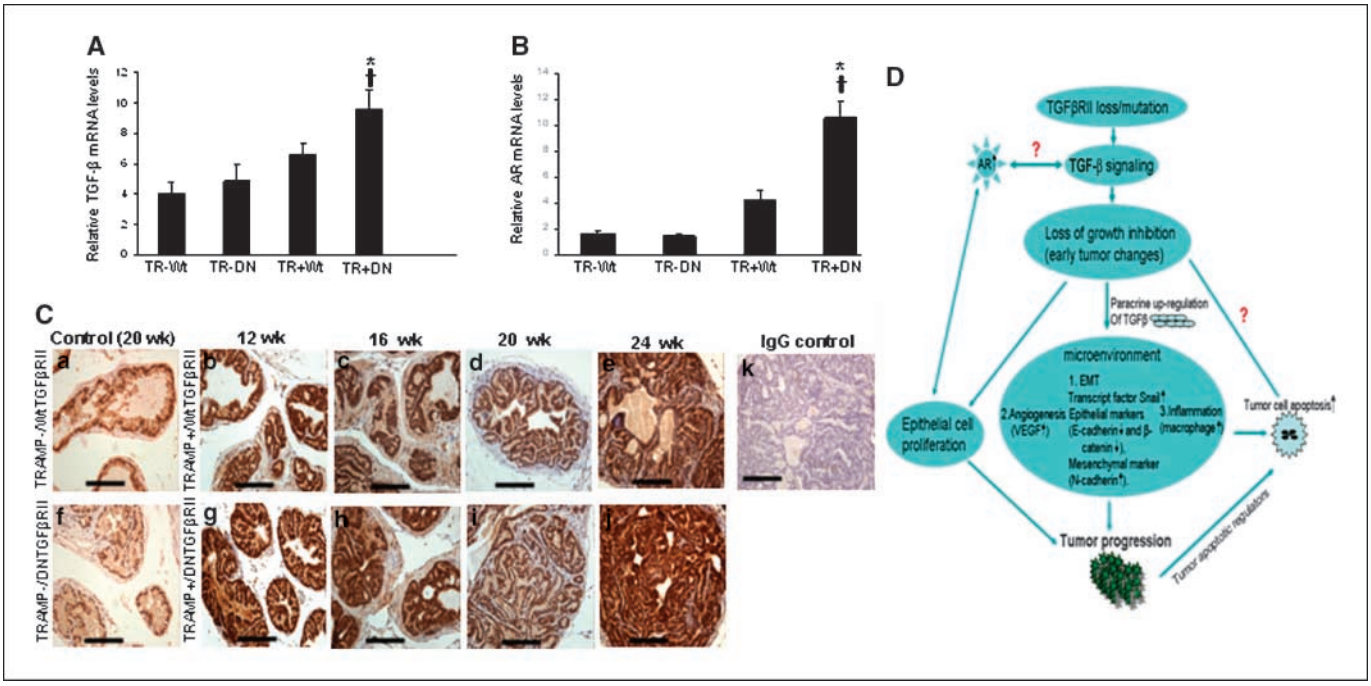

Figure 5. *A,* TGF-β and AR expression targeted in prostates from TRAMP+/DNTGFβRII+, TRAMP+/WtTGFβRII mice (20 wk). TGF-β ligand mRNA levels were assessed in prostate specimens by real-time RT-PCR. *, significant difference; †, values in TRAMP+/DNTGFβRII+ mice significantly different compared with controls. *B,* AR mRNA expression in prostates from TRAMP+/DNTGFβRII+, TRAMP+/WtTGFβRII mice. *, significant difference; †, values in TRAMP+/DNTGFβRII+ mice significantly different compared with controls. *C,* AR immunoreactivity in prostate specimens from 12- to 24-wk-old mice. *a* and *f,* controls; *g, h, i,* and *j,* AR expression in age-matched TRAMP+/DNTGFβRII+ prostates. *k,* negative control. *D,* impact of TGFβRII signaling loss on prostate growth dynamics. TGF-β dysfunctional signaling has direct consequences on the microenvironment, promoting EMT, inflammation, and angiogenesis toward tumor progression.

(52) is causal to the metastatic process. Our findings support the EMT effect in impaired TGF-β signaling (reduction in E-cadherin and β-catenin and increased N-cadherin and Snail expression). Snail overexpression in epithelial cells causes their mesenchymal phenotype, via E-cadherin down-regulation (53), by binding to the E-cadherin promoter to repress its transcription (54). A mutant DNTGFβRII receptor can promote recruitment of monocytes/macrophages by the microenvironment, a significant observation considering that macrophages represent the major inflammatory component of tumor stroma (55). Lack of recruitment of macrophages at the tumor site leads to decreased tumorigenic growth (56); moreover, clinical evidence suggests a correlation between a high tumor infiltration of macrophages and a poor prognosis of prostate cancer patients (55). TGF-β directly induces chemotaxis of monocytes/macrophages or indirectly causes immigration of inflammatory cells in combination with other modulatory cytokines or chemokines such as MCP-1 (57), toward regulating tumor-infiltrating monocytes/macrophages (48, 58).

In our model, targeted functional inactivation of TGF-β signaling in TRAMP mice provides a new insight into the effect of loss of TGF-β responsiveness on tumorigenesis: both via direct effects on cell proliferation and EMT, and indirectly via ligand up-regulation with associated paracrine effects on the tumor microenvironment. The dominant-negative approach makes the dissection of individual contributions by each effector component to TGF-β signaling in cancer difficult, by rendering the microenvironment unpredictable. The interaction between TGF-β and AR can lead to potential new therapeutic options based on inhibition of vital exchanges between TGF-β, its receptors, and AR, in the context of EMT during prostate tumor progression (59). Targeted restoration of TGF-β response in early carcinogenesis might constitute a potential therapeutic strategy for prostate cancer.

Disclosure of Potential Conflicts of Interest

No potential conflicts of interest were disclosed.

Acknowledgments

Received 2/27/09; revised 6/9/09; accepted 6/24/09; published OnlineFirst 9/8/09.

Grant support: NIH R01 Grant DK5355-12 (N. Kyprianou) and a UPR Summer Research Grant in Toxicology (J. Collazo). D. Gayheart is a University of Kentucky College of Medicine Clinical Research Scholar.

The costs of publication of this article were defrayed in part by the payment of page charges. This article must therefore be hereby marked *advertisement* in accordance with 18 U.S.C. Section 1734 solely to indicate this fact.

We thank Menglei Zhu for useful discussions and Lorie Howard for her assistance with the submission.

References

1. Jemal A, Siegel R, Ward E, et al. Cancer statistics, 2008. CA Cancer J Clin 2008;58:71–96.
2. Debes JD, Tindall DJ. Mechanisms of androgen-refractory prostate cancer. N Engl J Med 2004;351:1488–90.
3. Feldman BJ, Feldman D. The development of androgen-independent prostate cancer. Nat Rev Cancer 2001;1:34–45.
4. van der Poel HG. Androgen receptor and TGFβ1/Smad signaling are mutually inhibitory in prostate cancer. Eur Urol 2005;48:1051–8.
5. Zeng L, Rowland RG, Lele SM, Kyprianou N. Apoptosis incidence and protein expression of p53, TGF-β receptor II, p27Kip1, and Smad4 in benign, premalignant, and malignant human prostate. Hum Pathol 2004;35:290–7.
6. Guo Y, Jacobs SC, Kyprianou N. Down-regulation of

protein and mRNA expression for transforming growth factor-β (TGF-β1) type I and type II receptors in human prostate cancer. Int J Cancer 1997;71:573–9.
7. Fusaro G, Dasgupta P, Rastogi S, Joshi B, Chellappan S. Prohibitin induces the transcriptional activity of p53 and is exported from the nucleus upon apoptotic signaling. J Biol Chem 2003;278:47853–61.
8. Ayala GE, Dai H, Tahir SA, et al. Stromal antiapoptotic paracrine loop in perineural invasion of prostatic carcinoma. Cancer Res 2006;66:5159–64.
9. Chesire DR, Ewing CM, Gage WR, Isaacs WB. *In vitro* evidence for complex modes of nuclear β-catenin signaling during prostate growth and tumorigenesis. Oncogene 2002;21:2679–94.
10. Tu WH, Thomas TZ, Masumori N, et al. The loss of TGF-β signaling promotes prostate cancer metastasis. Neoplasia (New York, NY) 2003;5:267–77.
11. Linja MJ, Savinainen KJ, Saramaki OR, Tammela TL, Vessella RL, Visakorpi T. Amplification and overexpression of androgen receptor gene in hormone-refractory prostate cancer. Cancer Res 2001;61:3550–5.
12. Chen CD, Welsbie DS, Tran C, et al. Molecular determinants of resistance to antiandrogen therapy. Nat Med 2004;10:33–9.
13. Hayes SA, Zarnegar M, Sharma M, et al. SMAD3 represses androgen receptor-mediated transcription. Cancer Res 2001;61:2112–8.
14. Kang HY, Huang KE, Chang SY, Ma WL, Lin WJ, Chang C. Differential modulation of androgen receptor-mediated transactivation by Smad3 and tumor suppressor Smad4. J Biol Chem 2002;277:43749–56.
15. Chipuk JE, Cornelius SC, Pultz NJ, et al. The androgen receptor represses transforming growth factor-β signaling through interaction with Smad3. J Biol Chem 2002;277:1240–8.
16. Derynck R, Zhang YE. Smad-dependent and Smad-independent pathways in TGF-β family signalling. Nature 2003;425:577–84.
17. Tang B, de Castro K, Barnes HE, et al. Loss of responsiveness to transforming growth factor β induces malignant transformation of nontumorigenic rat prostate epithelial cells. Cancer Res 1999;59:4834–42.
18. Guo Y, Kyprianou N. Overexpression of transforming growth factor (TGF) β1 type II receptor restores TGF-β1 sensitivity and signaling in human prostate cancer cells. Cell Growth Differ 1998;9:185–93.
19. Guo Y, Kyprianou N. Restoration of transforming growth factor β signaling pathway in human prostate cancer cells suppresses tumorigenicity via induction of caspase-1-mediated apoptosis. Cancer Res 1999;59:1366–71.
20. Greenberg NM, DeMayo F, Finegold MJ, et al. Prostate cancer in a transgenic mouse. Proc Natl Acad Sci U S A 1995;92:3439–43.
21. Gingrich JR, Barrios RJ, Foster BA, Greenberg NM. Pathologic progression of autochthonous prostate cancer in the TRAMP model. Prostate Cancer Prostatic Dis 1999;2:70–5.
22. Gingrich JR, Barrios RJ, Morton RA, et al. Metastatic prostate cancer in a transgenic mouse. Cancer Res 1996;56:4096–102.
23. Gingrich JR, Barrios RJ, Kattan MW, Nahm HS, Finegold MJ, Greenberg NM. Androgen-independent prostate cancer progression in the TRAMP model. Cancer Res 1997;57:4687–91.
24. Bottinger EP, Jakubczak JL, Roberts IS, et al. Expression of a dominant-negative mutant TGF-β type II receptor in transgenic mice reveals essential roles for TGF-β in regulation of growth and differentiation in the exocrine pancreas. EMBO J 1997;16:2621–33.
25. Palmiter RD, Sandgren EP, Koeller DM, Brinster RL. Distal regulatory elements from the mouse metallothionein locus stimulate gene expression in transgenic mice. Mol Cell Biol 1993;13:5266–75.
26. Garrison JB, Kyprianou N. Doxazosin induces apoptosis of benign and malignant prostate cells via a death receptor-mediated pathway. Cancer Res 2006;66:464–72.
27. Suttie A, Nyska A, Haseman JK, Moser GJ, Hackett TR, Goldsworthy TL. A grading scheme for the assessment of proliferative lesions of the mouse prostate in the TRAMP model. Toxic Pathol 2003;31:31–8.
28. Bello-DeOcampo D, Tindall DJ. TGF-βl/Smad signaling in prostate cancer. Curr Drug Targets 2003;4:197–207.
29. Shi Y, Massague J. Mechanisms of TGF-β signaling from cell membrane to the nucleus. Cell 2003;113:685–700.
30. Brattain MG, Ko Y, Banerji SS, Wu G, Willson JK. Defects of TGF-β receptor signaling in mammary cell tumorigenesis. J Mammary Gland Biol Neoplasia 1996;1:365–72.
31. Massague J, Blain SW, Lo RS. TGFβ signaling in growth control, cancer, and heritable disorders. Cell 2000;103:295–309.
32. Kim SJ, Im YH, Markowitz SD, Bang YJ. Molecular mechanisms of inactivation of TGF-β receptors during carcinogenesis. Cytokine Growth Factor Rev 2000;11:159–68.
33. Akhurst RJ, Derynck R. TGF-β signaling in cancer-a double-edged sword. Trends Cell Biol 2001;11:S44–51.
34. Barcellos-Hoff MH, Medina D. New highlights on stroma-epithelial interactions in breast cancer. Breast Cancer Res 2005;7:33–6.
35. Barrett JM, Rovedo MA, Tajuddin AM, et al. Prostate cancer cells regulate growth and differentiation of bone marrow endothelial cells through TGFβ and its receptor, TGFβRII. Prostate 2006;66:632–50.
36. Albertsen PC, Hanley JA, Fine J. 20-year outcomes following conservative management of clinically localized prostate cancer. JAMA 2005;293:2095–101.
37. Potters L, Morgenstern C, Calugaru E, et al. 12-year outcomes following permanent prostate brachytherapy in patients with clinically localized prostate cancer. J Urol 2005;173:1562–6.
38. Roth BJ. Prostate cancer chemotherapy: emerging from the shadows. J Clin Oncol 2005;23:3302–3.
39. Shah RB, Mehra R, Chinnaiyan AM, et al. Androgen-independent prostate cancer is a heterogeneous group of diseases: lessons from a rapid autopsy program. Cancer Res 2004;64:9209–16.
40. Mohler JL, Gregory CW, Ford OH 3rd, et al. The androgen axis in recurrent prostate cancer. Clin Cancer Res 2004;10:440–8.
41. Taplin ME, Balk SP. Androgen receptor: a key molecule in the progression of prostate cancer to hormone independence. J Cell Biochem 2004;91:483–90.
42. Dehm SM, Tindall DJ. Molecular regulation of androgen action in prostate cancer. J Cell Biochem 2006;99:333–44.
43. Wang G, Sadar MD. Amino-terminus domain of the androgen receptor as a molecular target to prevent the hormonal progression of prostate cancer. J Cell Biochem 2006;98:36–53.
44. Song K, Wang H, Krebs TL, Kim SJ, Danielpour D. Androgenic control of transforming growth factor-β signaling in prostate epithelial cells through transcriptional suppression of transforming growth factor-β receptor II. Cancer Res 2008;68:8173–82.
45. Qi W, Gao S, Wang Z. Transcriptional regulation of the TGF-β1 promoter by androgen receptor. Biochem J 2008;416:453–62.
46. Zhu ML, Partin JV, Bruckheimer EM, Strup SE, Kyprianou N. TGF-β signaling and androgen receptor status determine apoptotic cross-talk in human prostate cancer cells. Prostate 2008;68:287–95.
47. Buck MB, Fritz P, Dippon J, Zugmaier G, Knabbe C. Prognostic significance of transforming growth factor β receptor II in estrogen receptor-negative breast cancer patients. Clin Cancer Res 2004;10:491–8.
48. Massague J. TGFβ in cancer. Cell 2008;134:215–30.
49. Forrester E, Chytil A, Bierie B, et al. Effect of conditional knockout of the type II TGF-β receptor gene in mammary epithelia on mammary gland development and polyomavirus middle T antigen induced tumor formation and metastasis. Cancer Res 2005;65:2296–302.
50. Scopa CD, Tsamandas AC, Zolota V, Kalofonos HP, Batistatou A, Vagianos C. Potential role of bcl-2 and ki-67 expression and apoptosis in colorectal carcinoma: a clinicopathologic study. Digest Diseases Sci 2003;48:1990–7.
51. Jaggi M, Johansson SL, Baker JJ, Smith LM, Galich A, Balaji KC. Aberrant expression of E-cadherin and β-catenin in human prostate cancer. Urol Oncol 2005;23:402–6.
52. Christofori G. New signals from the invasive front. Nature 2006;441:444–50.
53. Cano A, Perez-Moreno MA, Rodrigo I, et al. The transcription factor snail controls epithelial-mesenchymal transitions by repressing E-cadherin expression. Nat Cell Biol 2000;2:76–83.
54. Arias AM. Epithelial mesenchymal interactions in cancer and development. Cell 2001;105:425–31.
55. Balkwill F, Mantovani A. Inflammation and cancer: back to Virchow? Lancet 2001;357:539–45.
56. Lin EY, Li JF, Gnatovskiy L, et al. Macrophages regulate the angiogenic switch in a mouse model of breast cancer. Cancer Res 2006;66:11238–46.
57. Wrzesinski SH, Wan YY, Flavell RA. Transforming growth factor-β and the immune response: implications for anticancer therapy. Clin Cancer Res 2007;13:5262–70.
58. Umemura N, Saio M, Suwa T, et al. Tumor-infiltrating myeloid-derived suppressor cells are pleiotropic-inflamed monocytes/macrophages that bear M1- and M2-type characteristics. J Leukoc Biol 2008;83:1136–44.
59. Niu Y, Altuwaijri S, Lai KP, et al. Androgen receptor is a tumor suppressor and proliferator in prostate cancer. Proc Natl Acad Sci U S A 2008;105:12182–7.